

*This paper was recommended for publication in revised form by Editor in Chief Ahmet Selim Dalkilic*

## **STABILITY OF TURBINE BLADES, AIRCRAFT WINGS AND THEIR ACOUSTIC RADIATION**

Hamadiche Mahmoud  
Laboratoire de mécanique des fluides et d'acoustique  
36 av. Guy de Collongue, Ecully, 60139, France

*Keywords: Aeroelasticity, wing stability, noise generation, vibration control*  
*\* Corresponding author: Hamadiche Mahmoud, Phone: +330472448094*  
*E-mail address: mahmoud.hammadich@gmail.com*

### **ABSTRACT**

The stability of the wing is revisited in this work, the natural modes of the thin wing in incidence under the action of aerodynamic forces are calculated. The wing in this study has two degrees of freedom corresponding to the bending and torsion. Boundary between stable and instable zone are calculated. Wing stabilization by piezoelectric material are considered. The noise level produced by unsteady impinging gust is predicted.

### **INTRODUCTION**

The airfoils and blades are involved in many applications nowadays, wind turbine, commercial air planes, turbines, compressor, fans, rotors and propellers are not the unique examples. The flow around an airfoil and blade depends on the geometrical configuration of the airfoil and the nature of the flow in far field. For a stable wing of small angle of attack the flow is attached to the wing and the oscillation of the lift and consequently the vibration of the wing are mainly imposed by turbulence density of far field free stream. When the angle of attack exceeds its critical values the flow is no longer attached to the wing and the flow separation occurs, a phenomenon associated with a dramatic fall on the lift. If the angle of attack is increased farther the wing behave like a bluff body generating a structure similar to the classic Kármán vortex street. The frequency of the shedding vortex increases with the increase of the free stream velocity and decreases with the increase of the angle of attack and the amplitude of the oscillation are lock-in with the frequency of shedding vortex [3,4].

The flow around a thick airfoil is shown to be controllable by a blowing from a slot located in the leading

edge. Airfoil stall can be either promoted or inhibited depending on the momentum of jet's slot and a corresponding reduction or increase in the lift is obtained [5, 6]. This technique is in great interest in wind turbine in order to achieve constant energy supply.

The numerical and experimental analysis of the flow around a sickle-shaped planform shows that the spanwise varying mean flow has an important effects on the stability of the field flow around the airfoil leading to the development of crossflow vortices in addition to the classical Tollmien-Schlichting one [7,8], which leads to move the transition location upstream. A dynamic mode decomposition technique and a proper orthogonal decomposition technique are applied to analyze the unsteady flow field around stalling angle of attack of airfoil. Numerically obtained velocity as well as experimentally obtained one are considered for the analysis, it is shown the imprecision attached to the experimental measurement near the rigid surface has a moderate effect on the obtained modes [9,10,11].

In some circumstances, the airfoil can be subjected to different flight conditions as it is the case in tilt-rotor aircraft for instance, where the airfoil has to function in hovering helicopter mode as well as as a propeller in forward flight. In hover flight mode more power is needed to overcome the weight of the helicopter, while in forward flight mode the plane wing support and balance the weight of the plane, therefore the power needed is only to overcome the resistance of the air to the advancement of the plane. The optimal angle of attack for the two mentioned flight regimes is not the same and the rotor has to accommodate by changing its rotation speed or its angle of attack. Therefore, a advanced composite material is needed

to obtain aeroelastic responses favorable for the stability and the performance of tilt-rotor engine [12].

Controlled strain-induced blade twisting can be attained using piezoelectric active fiber composite technology, aimed at provide a mechanism for reducing rotorcraft vibrations and increasing rotor performance [13]. An optimization technique is proposed in order to select the optimal design variables like the thickness of each composite layer, center of gravity of the cross section, shear center, mass per unity length, cord and ballast mass allowing optimal active twist rotors [14]. A passive control strategy for blades disk interaction in compressor and turbine using piezoelectric shunt damping technique is feasible, the strategy is to place the piezoelectric transducers outside the main stream in turbo machinery so that the flow is not perturbed [15], and an optimization technique is employed in order to place the piezoelectric shunt at optimal locations [15]. In the case of a high aspect ratio low-pressure turbine blade the unstable bladed disk reaches a state in which only a single traveling wave exists [16]. A full wing-fuselage coupling with rigid-body roll degree of freedom for fuselage and elastic modes for the wing is investigated by both numerical and experimental technique. It is found that the post flutter response is a limit-cycle oscillation [17]. An experimental method and numerical technique are developed to apprehend the transient response of multilayer composite rotating airfoil under a slicing-impact loading and birdlike struck is investigated [18, 19]

Flutter instability can be used to harvest energy for small electric devises. The wing parameters are chosen so that it is becomes instable with respect to flutter instability. Then piezoelectric transducer is introduced to transform the persistent oscillation of the wing in order to harvest energy for electrical devises [20].

Experimental evidence shows that a propeller ingestion turbulence is a source harmful noise [21, 22, 23]. An analytical approach, based on two points correlations technique of unsteady axial and radial forces exerted on a rotor, is shown to be an adequate model to predict acoustic radiation of a rotor ingestion turbulence, a satisfactory agreement between analytically obtained results and experimental ones has been reported [24]. Experimental evidence shows that axial-flows in fans, compressors, turbines are source of discrete-frequency sound radiation. The sound radiation is induced by forces fluctuation in either a rotor or a stator stage due to interaction with upstream component. A fundamental forward step in the comprehension of acoustic radiation in turbo-machinery is to have insight on the mechanism of acoustic radiation due to a gust impinging stator blade, rotor blade and airfoil. Acoustics methods include analytical, semi-analytical, numerical techniques and experimental technique to predict the sound propagation and radiation are developed in the literature. Nonreflecting boundary conditions for the time dependent Euler equation are shown to be necessary for predicting acoustic radiation [25,26, 27]. Active control of rotor-stator interaction noise using stator-mounted actuator are showing to be an efficient method for noise reduction. It has been shown that a

reduction in noise as far as 50% can be reached in efficient control [28].

**FLOW AROUND THIN WING**

In the following we shall develop a mathematical model to study the stability of an elastic wing and its acoustic radiation. The wing is assumed to be sufficiently thin and slightly curved such that the wing chord can be confused with the z axis, as is shown schematically in Figure 1. Let R (o, x, y, z) be a reference frame attached to the wing, so that the leading edge is the origin of coordinates, figures 1. The wing is then in the interval [0, c]. c is the chord of the wing. Let a continuous vorticity of density  $\gamma$  located on the chord (in this case about the z axis), then the potential flow generated by the presence of the wing is given by the following improper integral

$$f = - (1/2\pi) \int \gamma(z_0) \text{Arctan} (y/(z-z_0)) dz_0 \tag{1}$$

where  $\gamma(z_0)$  is the density of the vorticity at  $z_0$ . Let  $(v_y, v_z)$  be the velocity components in y and z directions, respectively. By definition of the flow potential, the velocity components are

$$v_y = \partial f / \partial y \quad ; \quad v_z = \partial f / \partial z. \tag{2}$$

Let  $U_\infty$  be the velocity of the flow far from the wing and  $\theta$  is the angle of incidence of the wing. The speed of the flow in the vicinity of the wing is then  $v = [v_y + U_\infty \sin(\theta), v_z + U_\infty \cos(\theta)]$ .  $\gamma$  depends on the incidence angel  $\theta$ , on the displacement of the wing denoted w, on the curvature of the wing and on the geometrical and rheological parameters of the wing and the fluid.

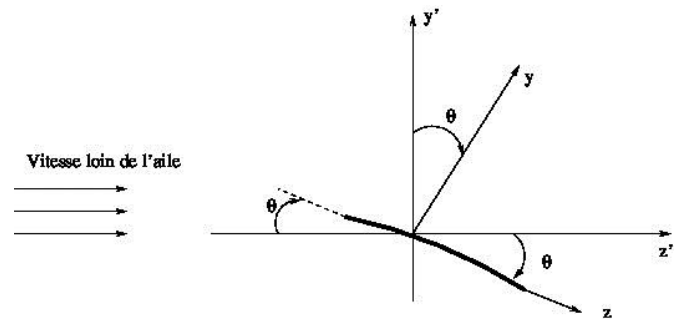


Figure 1. Configuration of the system

**PRESSURE AT THE WING SURFACE**

The velocity field in the vicinity of the wing is

$$v = [v_y + U_\infty \sin(\theta), v_z + U_\infty \cos(\theta)] \tag{3}$$

so,

$$v^2 = U_\infty^2 + v^2 + 2 v_y \sin(\theta) U_\infty + 2 v_z \cos(\theta) U_\infty \tag{4}$$

using Bernoulli's theory and neglecting the quadratic terms, the pressure can be approximated by the equation

$$p = -\rho U_\infty v_z \quad (5)$$

For the previous expression we considered the ambient pressure as a reference pressure and we have neglected terms of order two. It is assumed that  $\theta \ll 1$ ,  $v_y \ll U_\infty$  and  $v_z \ll U_\infty$ . Using the approximation of then airfoil, in the vicinity of the wing, the pressure on the upper surface of the wing,  $p(0^+, z)$ , and the pressure in lower surface of the wing  $p(0^-, z)$  are

$$p(0^+, z) = -\rho U_\infty \gamma(0^+, z)/2, \quad (6)$$

$$p(0^-, z) = \rho U_\infty \gamma(0^-, z)/2, \quad (7)$$

$\gamma(0^+, z)$  and  $\gamma(0^-, z)$  can be calculated using the impermeability condition at the wing surface. For a thin wing we have  $\gamma(0^+, z) = \gamma(0^-, z) = \gamma(z)$ . The pressure is used to calculate the aerodynamic forces on the wing. Thus, the lift is

$$f = \int (p(0^-, z) - p(0^+, z)) dz = \rho U_\infty \int \gamma(z) dz \quad (8)$$

where  $z$  is in the interval  $[0, c]$ ,  $c$  is the airfoil chord, and the moment at the edge of the wing is

$$m(o) = -\rho U_\infty \int z \gamma(z) dz. \quad (9)$$

where  $\gamma(z)$  is supposed to be of the form

$$\gamma(\beta) = 2U_\infty \{A_0[1 + \cos(\beta)]/\sin(\beta) + A_n \sin(n\beta)\} \quad (10)$$

where the convention on the summation over the repeated indices are used,  $\beta$  is such that

$$z = (c/2)[1 - \cos(\beta)]. \quad (11)$$

The moment  $m_e$  on the shear axis can be obtained by the transport connection. Under the precedent condition, the lift and the moment on shear axis are

$$f = \rho \pi U_\infty^2 c [\theta - (L-3c/4) \partial \theta / \partial t / U_\infty - \partial w / \partial t / U_\infty] \quad (12)$$

$$m_e = \rho \pi U_\infty^2 c^2 \{(1/4 - L/c) [\theta + (cL) \partial \theta / \partial t / U_\infty - \partial w / \partial t / U_\infty] + L \partial \theta / \partial t / (4U_\infty)\} \quad (13)$$

where  $c$  stands for the chord of the wing,  $L$  stands for the distance between the leading edge and the shear axis,  $\rho$  stands for the fluid density and  $t$  stands for time.

### WING MODEL

The wing is considered as a beam under coupled torsion and flexion whose movement is governed by the following equations:

$$EI \partial^4 w / \partial x^4 + \rho_s S (\partial^2 w / \partial t^2 - z_\alpha \partial^2 \theta / \partial t^2) = f \quad (14)$$

$$I_\alpha \partial^2 \theta / \partial t^2 - \rho_s S z_\alpha \partial^2 w / \partial t^2 = m_e + GJ \partial^2 \theta / \partial x^2 \quad (15)$$

The lift  $f(w, \theta)$  and the aerodynamic moment  $m_e(w, \theta)$  are given by equation (12)-(13). In the above equation,  $z_\alpha$  is the distance between the shear axis and the center of the mass,  $S$  is the section of the wing,  $\rho_s$  is the mass density of the wing,  $G$  is the shear modulus,  $E$  is the Young's modulus,  $I, I_\alpha$  and  $J$  are the moments of inertia of the cross section. The boundary conditions associated with the above equations are at  $x = 0$

$$\theta = w = \partial w / \partial x = 0 \quad (16)$$

and at  $x = l$

$$\partial \theta / \partial x = \partial^2 w / \partial x^2 = \partial^3 w / \partial x^3 = 0. \quad (17)$$

This condition indicates the absence of the forces and moment on the wing tip.

### NUMERICAL METHOD

The solution of the system of partial differential equations is sought in the form of a normal mode, i.e.

$$[w(x, t), \theta(x, t)] = [w_\omega(x, \omega), \theta_\omega(x, \omega)] e^{i\omega t}. \quad (18)$$

where the equation of motion become

$$EI d^4 w_\omega / dx^4 + \rho_s S (-\omega^2 w_\omega + \omega^2 z_\alpha \theta_\omega) = f_\omega \quad (19)$$

$$-\omega^2 I_\alpha \theta_\omega + \omega^2 \rho_s S z_\alpha w_\omega = m_{e\omega} + GJ d^2 \theta_\omega / dx^2 \quad (20)$$

and the boundary conditions at  $x=0$  are

$$\theta_\omega = w_\omega = dw_\omega / dx = 0, \quad (21)$$

and  $x = l$  are

$$d\theta_\omega / dx = d^2 w_\omega / dx^2 = d^3 w_\omega / dx^3 = 0. \quad (22)$$

The aerodynamic external forces are then

$$f_\omega = \rho \pi U_\infty^2 c [\theta_\omega - i\omega (L-3c/4) \theta_\omega / U_\infty - i\omega w_\omega / U_\infty], \quad (23)$$

$$m_{e\omega} = \rho \pi U_\infty^2 c^2 \{(1/4 - L/c) [\theta_\omega + i\omega (c-L) \theta_\omega / U_\infty - i\omega w_\omega / U_\infty] + i\omega L \theta_\omega / (4U_\infty)\}. \quad (24)$$

The previous system is solved by fourth-order Runge-Kutta method. By choosing appropriate boundary conditions at  $x = 0$ , it is possible to find numerically 3 linearly independent solutions, denoted  $X_1=(w_{1\omega}, \theta_{1\omega})$ ,  $X_2=(w_{2\omega}, \theta_{2\omega})$ ,  $X_3=(w_{3\omega}, \theta_{3\omega})$ . The linear independence of these solutions is provided by an orthogonal choice of the boundary conditions imposed on the derivative of  $\theta$ , the second derivative of  $w$  and the third derivative of  $w$  at  $x=0$ . The general solution of the problem is a linear combination of these three solutions, thus,

$$X = A_1 X_1 + A_2 X_2 + A_3 X_3 \tag{25}$$

$A_1, A_2$  and  $A_3$  are arbitrary constant. The constructed solution satisfies the boundary conditions at  $x=0$ . The  $X$  solution must satisfy the boundary conditions at  $x = l$  which leads to the following equations

$$A_1 d\theta_{1\omega}/dx + A_2 d\theta_{2\omega}/dx + A_3 d\theta_{3\omega}/dx = 0, \text{ at } x = l \tag{26}$$

$$A_1 d^2 w_{1\omega} / dx^2 + A_2 d^2 w_{2\omega} / dx^2 + A_3 d^2 w_{3\omega} / dx^2 = 0, \text{ at } x = l \tag{27}$$

$$A_1 d^3 w_{1\omega} / dx^3 + A_2 d^3 w_{2\omega} / dx^3 + A_3 d^3 w_{3\omega} / dx^3 = 0, \text{ at } x = l, \tag{28}$$

the previous system can be written in a concise form, thus,

$$MA = 0, \tag{29}$$

where  $M$  is a matrix whose components are the constant coefficient of the unknown variables  $A_i, i = 1,2,3$  of the above system which are numerically identified, and  $A = (A_1, A_2, A_3)$ . The system shall admits a no trivial solution if and only if the determinant of  $M$  is zero, that is  $D = \det(M) = 0$ . The equation  $D=0$  has a solution for some values of  $\omega$ , the values of  $\omega$  which satisfy equation  $D = 0$ , are the eigenvalues of the system.  $\omega$  is the complex number,  $\omega = \omega_r + i \omega_i$ . The system is unstable if and only if  $\omega_i < 0$ ,  $\omega$  depends on the parameters of the system, i.e.  $\omega(E, G, U_\infty, \dots)$ . The equation of critical curves defining boundary of stable and unstable zones in the control parameters planes are

$$D(G, U_\infty, \dots) = 0 \text{ and } \omega_i(G, U_\infty, \dots) = 0. \tag{30}$$

For example, the values of  $G$  and  $U_\infty$  which are the roots of the two above equations form a critical curve in  $(G, U_\infty)$  plane. The roots of the two above equation are obtained by an iterative method, namely, the secant method.

**Boundary between stable and unstable zone**

Figure 2 shows the values of two unstable modes versus the speed of the aircraft, all the other wing parameters are kept constant. The figure shows that the wing becomes unstable when the speed is higher than  $\approx 281 \text{ m/s}$  for the

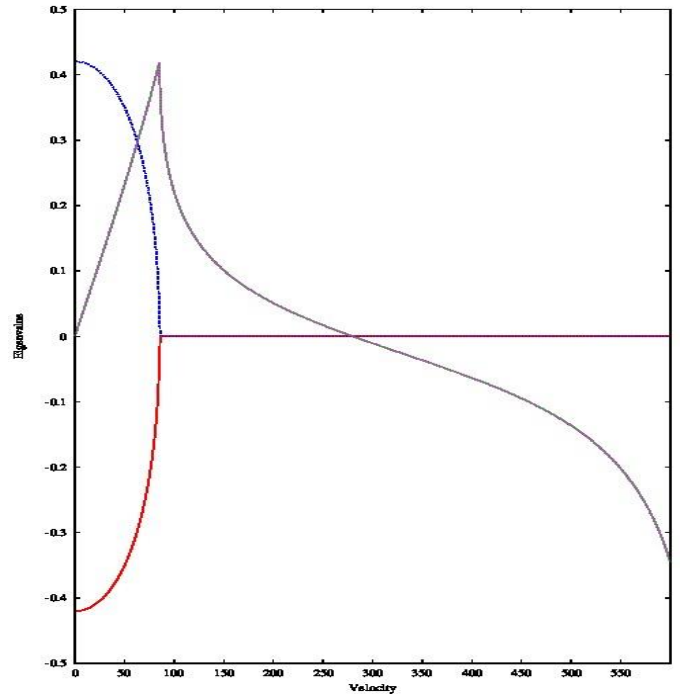


Figure 2. Eigenvalues versus the velocity of the airfoil. The blue and the red curves are the frequency and third curve is the amplification rate.

selected configuration here. Figure 3 shows the critical curves in the plane  $(L, U_\infty)$  for different values of the shear modulus of the wing. It found that the wing is stable as far as  $L < C/4$ . However,  $L$  can exceed this value for large  $G$ .

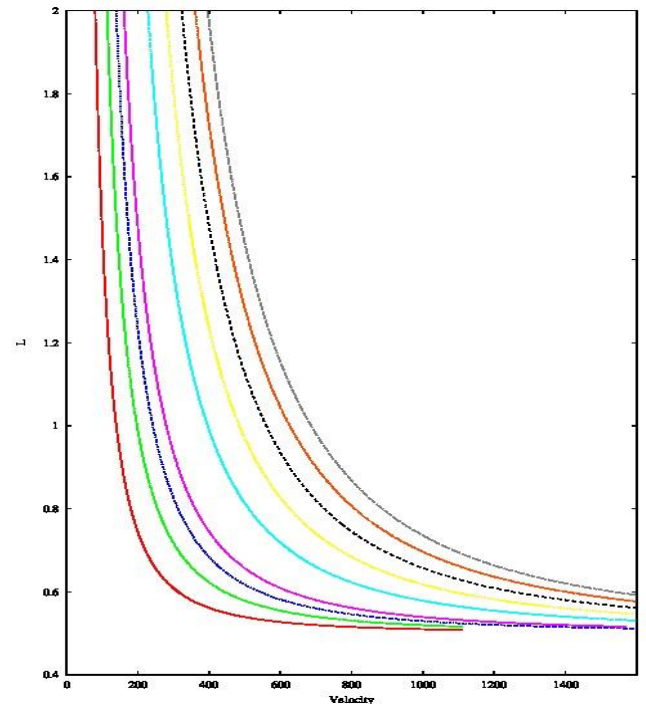


Figure 3. Instability boundary in the plan  $(L, U_\infty)$  for some shear modulus,  $L$  is the shear axis position and  $U_\infty$  is speed of the wing. The zone above the curves are instable.

**Passive piezoelectric shunt damping techniques**

Vibration control based on the passive piezoelectric shunt damping technique has been documented in the literature [15]. In this paragraph, we shall present an example to show how piezoelectric shunt can be used to delay the threshold instability of blade of airfoil. Let some piezoelectric material be inserted in the wing or in the blade, so that the wing motion is coupled to two electrical circuit powered by the piezoelectric material, the equation of motion become,

$$EI\partial^4 w / \partial x^4 + \rho_s S (\partial^2 w / \partial t^2 - z_\alpha \partial^2 \theta / \partial t^2) - K_1 q_1 = f \tag{31}$$

$$I_\alpha \partial^2 \theta / \partial t^2 - \rho_s S z_\alpha \partial^2 w / \partial t^2 - K_2 q_2 = m_e + GJ \partial^2 \theta / \partial x^2 \tag{32}$$

$$L_1 d^2 q_1 / dt^2 + R_1 dq_1 / dt - K_1 \partial w / \partial t = 0, \tag{33}$$

$$L_1 d^2 q_2 / dt^2 + R_2 dq_2 / dt - K_2 \partial \theta / \partial t = 0. \tag{34}$$

where the two constant  $K_1$  and  $K_2$  are reflecting the electromechanical coupling effects,  $L_1$  and  $L_2$ ,  $R_1$  and  $R_2$ , are the inductances of and the resistances of the two electrical circuits respectively. The solution of the system of partial differential equations is sought in the form of a normal mode, i.e.

$$[w, \theta, q_1, q_2] = [w_\omega, \theta_\omega, q_1^\omega, q_2^\omega] e^{i\omega t}. \tag{35}$$

The equation of motion become

$$EI d^4 w_\omega / dx^4 + \rho_s S (-\omega^2 w_\omega + \omega^2 z_\alpha \theta_\omega) - K_1 q_1^\omega = f_\omega \tag{36}$$

$$-\omega^2 I_\alpha \theta_\omega + \omega^2 \rho_s S z_\alpha w_\omega - K_2 q_2^\omega = m_{e\omega} + GJ d^2 \theta_\omega / dx^2 \tag{37}$$

where  $f_\omega$  and  $m_{e\omega}$  are as in equations 21 and 22.

$$-\omega^2 L_1 q_1^\omega + i\omega R_1 q_1^\omega - iK_1 \omega w_\omega = 0, \tag{38}$$

$$-\omega^2 L_1 q_2^\omega + i\omega R_2 q_2^\omega - iK_2 \omega \theta_\omega = 0. \tag{39}$$

In the numerical investigation of this paragraph a particular case is treated here. In that we neglect the effects of flexion, namely,  $w=0$ , and we consider only equations (20) and (34) which involve the variation of pithing angle coupled to the electrical circuit. Ignoring the effects of boundary conditions, a particular solution in the form  $\exp(ikx)$  has been sought.

Figure (4) shows the instable mode versus the speed the airfoil. The figure show that the system become instable when the speed exceeds some critical value. Figure (5) show how the threshold of the instability is delayed for some values of the coupling constant. The figure shows that the divergence instability can be efficiently removed by a strong coupling with piezoelectric material.

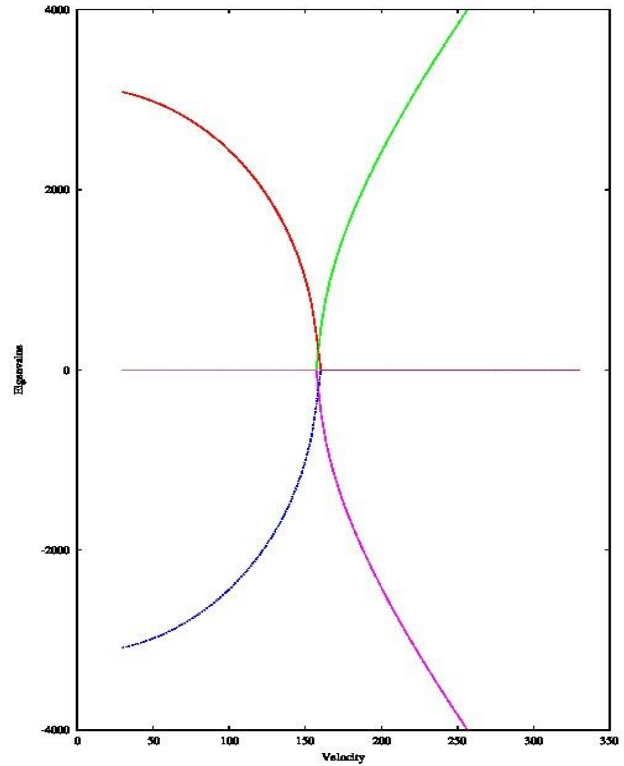


Figure 4. The eigenvalues values obtained after neglecting the flexion. The red and blue lines are the frequencies and the green and the magenta are the amplification rate

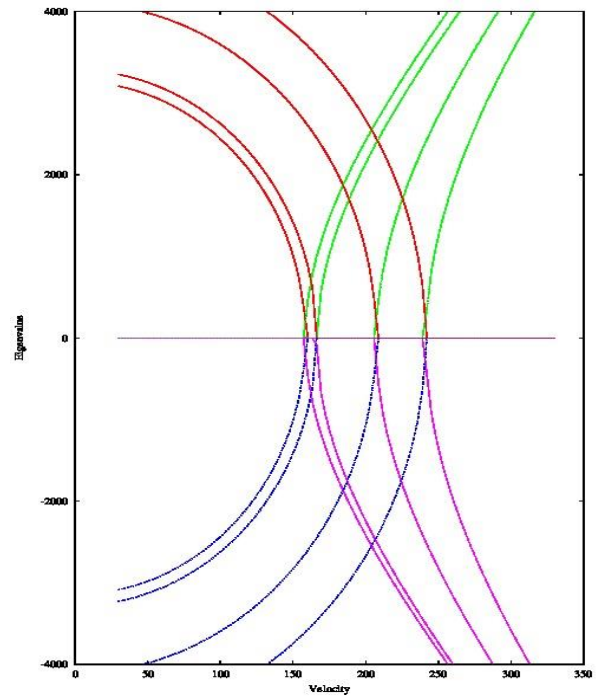


Figure 5. The eigenvalues obtained for some values of coupling constant with piezoelectric material. The caption as in figure 4. The figure shows that instability of the wing is delayed.

**Acoustic radiation of an impinging gust**

In this paragraph a rigid airfoil is considered in order to study acoustic radiation. The airfoil has an angle of incidence  $\alpha$ . Let's consider a sinusoidal gust superimposed to the far field mean flow so that the flow velocity far from the wing is

$$U_\infty = \{U_\infty + \varepsilon \cos[(U_\infty t + \delta z - \beta y)/a]\} \cos(\alpha) \mathbf{z} + \{U_\infty + \varepsilon \cos[(U_\infty t + \delta z - \beta y)/a]\} \sin(\alpha) \mathbf{y} \quad (40)$$

$\delta = \sin(\alpha)$  and  $\beta = \cos(\alpha)$  so that the velocity in the far field is a divergence free,  $a$  is a characteristic length of the incoming gust and  $\varepsilon$  is the amplitude of the incoming gust.  $\alpha$  is supposed to be small enough so that

$$\sin(\alpha) \approx \alpha \text{ and } \cos(\alpha) \approx 1 \quad (41)$$

Let  $(0, v_y, v_z)$  be the perturbation induced by the thin airfoil, using the boundary condition at the surface of the thin airfoil lead to the equation

$$v_y = \{U_\infty + \varepsilon \cos[(U_\infty t + \delta z - \beta y)/a]\} [d\eta/dz - \alpha] \quad (42)$$

which must be hold at the surface of the airfoil,  $\eta$  is the position of the airfoil cord in the plan  $(o, y, z)$ . In order to find  $\gamma(z)$ , the following equation has be solved, that is

$$v_y = \{U_\infty + \varepsilon \cos[(U_\infty t + \delta z - \beta y)/a]\} [d\eta/dz - \alpha] = -(1/2\pi) \int \gamma(z_0) \{ (z-z_0)/[(z-z_0)^2 + y^2] \} dz_0 \quad (43)$$

The steady part of the equation is not relevant as far as the acoustic radiation is of interest, therefore we cancel it from the above equation so that at first order one has to solve the following integral equation

$$\{ \varepsilon \cos[(U_\infty t + \delta z - \beta y)/a] \} \alpha = -(1/2\pi) \int \gamma(z_0) \{ (z-z_0)/[(z-z_0)^2 + y^2] \} dz_0 \quad (44)$$

Using equation (10) and (11) and evaluate the integral for small  $y$  lead to the constants  $A_n$  thus

$$A_0 = -2 \alpha \varepsilon \cos[(U_\infty t + \alpha c/2)/a] \quad (45)$$

$$A_n = 0 \text{ if } n \text{ is even} \quad (46)$$

$$A_n = -\alpha \varepsilon (-1)^n J_n[\alpha c/(2a)] \sin[(U_\infty t + \alpha c/2)/a] \quad (47)$$

for  $n$  odd.  $J_n$  is Bessel function of order  $n$ . In the precedent calculation, the following relation is used

$$e^{iz \cos(\beta)} = i^n J_n e^{in \beta} \quad (48)$$

where the convention on the summation over the repeated indices are used,  $i = (-1)^{1/2}$  and  $n \in (-\infty, \infty)$ .

In order to estimate the acoustic radiation of the wing, the wave equation

$$\partial^2 p / \partial t^2 = v_c \Delta p \quad (49)$$

where  $v_c$  is the speed of sound and  $p$  is the acoustic pressure.

The solution is obtained with the following hypothesis. The acoustic pressure at the surface of the airfoil is equal to the unsteady pressure induced by the incoming gust at the surface of the wing. The derivative of the acoustic pressure in the direction of the normal to the surface of the wing is null. Let  $G$  be the Green function of the wave equation, the solution of the wave equation is then

$$p = - \int^{t^+} d\tau \int ds_0 p \partial G(\tau, \mathbf{r}, \mathbf{r}_0) / \partial n_0 \quad (50)$$

$s_0$  is the surface of the airfoil and  $\tau$  stands for time. It is very well knowing that

$$G(\tau, \mathbf{r}, \mathbf{r}_0) = G(\tau, R) = \delta(R/v_c - t) / R^2, \quad (51)$$

$$R = [(x-x_0)^2 + (y-y_0)^2 + (z-z_0)^2]^{1/2} \quad (52)$$

and  $\delta$  is Dirac function. At the upper surface of the wing,

$$\partial G(\tau, R) / \partial n_0 = \partial G(\tau, R) / \partial y_0 \quad (53)$$

and at lower surface of the wing

$$\partial G(\tau, R) / \partial n_0 = -\partial G(\tau, R) / \partial y_0 \quad (54)$$

therefore the solution of the wave equation becomes

$$p = - \int^{t^+} d\tau \int ds_0 (p(0^+, t, z_0) - p(0^-, t, z_0)) \partial G(\tau, R) / \partial y_0 = \rho U_\infty \int ds_0 \gamma(t, z_0) \partial G(\tau, R) / \partial y_0 \quad (55)$$

using the the explicit expression of Green function and knowing that,

$$\partial G(\tau, R) / \partial y_0 = \partial G(\tau, R) / \partial R \partial y_0 = 2(y-y_0) \delta(R/v_c - t) / R^3 \quad (56)$$

we get

$$p = 2\rho U_\infty \int ds_0 \gamma(R/v_c, z_0) ((y-y_0) / R^3) \quad (57)$$

where  $\gamma(R/v_c, z_0)$  is given by equation (10)-(11) and  $A_n$  are as in equation (45)-(47) where  $t$  is replaced by  $R/v_c$ .

**Far field approximation**

At large distance from the source, the displacement of  $\mathbf{r}_0$  upon the surface of the airfoil induces a negligible variation of  $R$ , therefore, during the integration over the surface of the wing  $R$  can be considered as constant. The integration of  $\gamma$  for  $R$  constant cancel all the term in the series (10) but  $A_0$  and  $A_1$ . Therefore, taking account to the fact that for large distance

$$((y-y_0) / R^3) \approx \sin(\xi) \sin(\zeta) / R^2 \quad (58)$$

equation (57) becomes

$$p = 2\rho\pi LcU_\infty^2 (A_0 + A_1/2)\sin(\theta)\sin(\phi)/R^2 \tag{59}$$

$\xi$  and  $z$  in equation (58) are the polar and the azimuthal angles in spherical coordinates of the frame  $R(o,x,y,z)$ . More explicitly, the acoustic pressure far from the source is

$$p = -4\rho\pi \varepsilon LcU_\infty^2 \{ \cos[(U_\infty R/v_c + \alpha c/2)/a] + J_1[\alpha c/(2a)] \sin[(U_\infty R/v_c + \alpha c/2)/a]/4 \} \sin(\xi)\sin(\zeta)/R^2 \tag{60}$$

Figures (6) - (7) show the level of noise in far field as function of the distance, the model does not include any arbitrary constant and the obtained noise level seems to be correct.

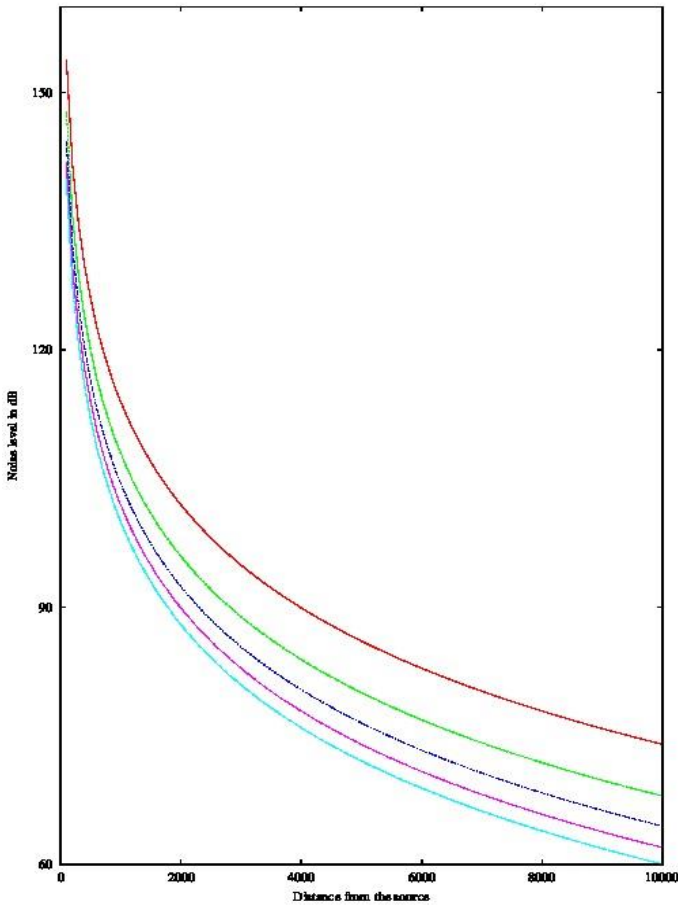


Figure 6. The level of noise in decibel versus the distance from the wing for some values of the amplitude of the impinging gust.

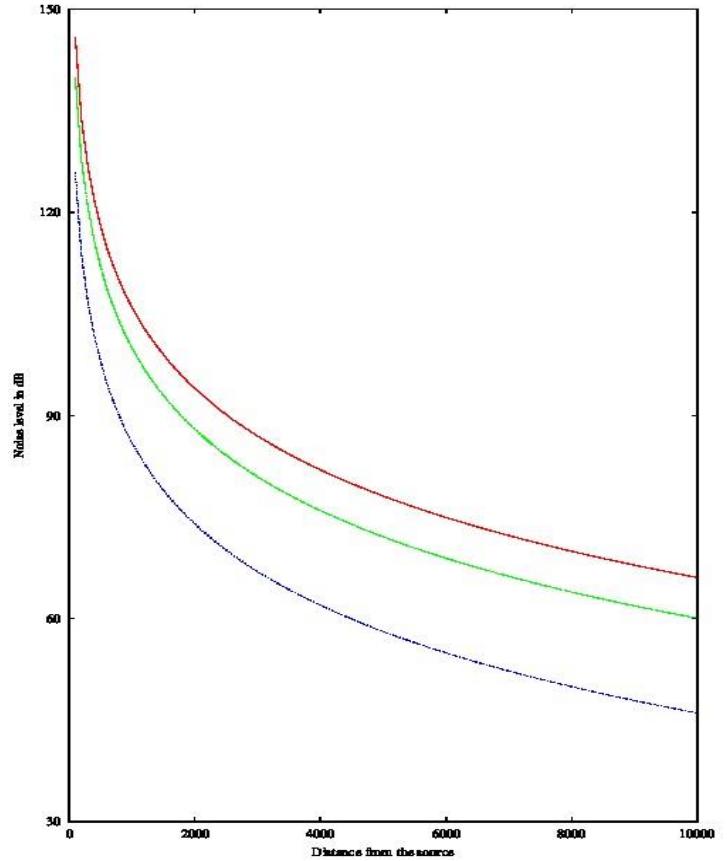


Figure 7. The level of noise in decibel versus the distance from the source for some values of the angle of incidence.

**CONCLUSION**

A model of the stability of an elastic airfoil is developed, the model is based in the first principal and does not include any arbitrary constant. It is shown that the instability of the wing depends on the position on the shear axis and that the instability of the airfoil can be delayed by adding to the wing piezoelectric material. A model of the wing's acoustic radiation is developed and the obtained noise level seems to be correctly predicted.

**REFERENCES**

[1] Fung, Y. C., 2002, "An introduction to the theory of aeroelasticity," *Dover Phoenix Editions*.  
 [2] Hamadiche, M., 2007, "Elastic wing's response to an incoming gust," *Int Jnl of multiphysics*, Vol. 1, Number 2.  
 [3] Tang, D. M., and Dowell, E. H., 2014, "Experimental aerodynamic response for an oscillating airfoil in buffeting flow," *AIAA journal*, Vol. 52, No. 6 June, pp. 2427-2439.  
 [4] Tang, D. M., and Dowell, E. H., 2007, "Aerodynamic loading for an airfoil with an oscillating Gurney flap," *AIAA journal*, Vol. 44, No. 4, pp. 1245-1257.

- [5] Müller-Vahl, H. F., 2015, "Control of thick airfoil, deep dynamic stall using steady blowing," *AIAA journal*, Vol. 53, No. 2, pp. 277-295.
- [6] Sasson, B. and Greenblatt, D., 2011, "Effect of leading-edge slot blowing on a vertical axis wind turbine," *AIAA journal*, Vol. 49, No. 9, pp. 1932-1942.
- [7] Petzold, R. and Radespiel, R., 2015, "Transition on a wing with spanwise varying crossflow and linear stability analysis," *AIAA journal*, Vol. 53, No. 2, pp. 321-335.
- [8] Bippes, H., 1999, "Basic Experiments on transition in three-dimensional boundary layers dominated by crossflow instability," *Progress in Aerospace Sciences*, Vol. 35, No. 4, pp. 363-412
- [9] Mariappan, S., Gardner, A. D. and Richter, A. D., 2014, "Analysis of dynamic stall using dynamic mode decomposition technique," *AIAA journal*, Vol. 52, No. 11, pp. 2427-2439.
- [10] Schmid, P. J., 2010, "Dynamic mode decomposition of numerical and experimental data," *Journal Fluid Mechanics*, Vol., 656, pp. 5-28.
- [11] Ekaterinaris, J. A. and Pllatzer, M. F., 1998, "Computational prediction of airfoil dynamic stall," *Progress in Aerospace Sciences*, Vol. 33, Nos. 11-12, pp. 759-846.
- [12] Nixon, M. W., Piatak, D. J., Corso, L. M. and Popelka D. A., 1999, "Aeroelastic tailoring for stability augmentation and performance enhancement of tiltrotor aircraft," American Helicopter Society 55th Annual forumm, Moterial, Quebec, Canada, Mai 25-27.
- [13] Wilbur, M. L., Mirick, P. H., Yeager, W. T., Langston, C. W., Cesnik, C.E. S. and Shin, S., 2002, "Vibratory Loads Reduction Testing of the NASA/Army/MIT Active Twist Rotor," *Journal of the American Helicopter Society*, Vol. 47, No. 2, pp. 123-133
- [14] Kumar, D. and Cesnik C. E. S., 2015, "New optimization strategy for design of active twist rotor," *AIAA journal*, Vol. 53, No. 2, pp. 436-448.
- [15] Zou, B. Thouverez, F. and Lenoir, D., 2014, "Vibration reductionb of mistuned bladed disk by passive piezoelectric shunt damping technique," *AIAA journal*, Vol. 52, No. 6, pp. 1194-1206.
- [16] Corral, R. and Gallardo, J. M., 2014, "Nonlinear dynamics of blade disk with multiple unstable modes," *AIAA journal*, Vol. 52, No. 6, pp. 1124-1132.
- [17] Tang, D. and Dowell E. H., 2014, "Effects of free-to-roll fuselage on wing flutter: theory and experiment," *AIAA journal*, Vol. 52, No. 12, pp. 2625-2632.
- [18] Gong, X., Bansmer, S. Strobach, Ch., Unger R. and Haupt M., 2014, "Deformation measurement of a birdlike aifoil with optical flow and numerical simulation," *AIAA journal*, Vol. 52, No. 12, pp. 2807-2816.
- [19] Sinha, S. 2014, "Transient response of a multilayered composite rotating airfoil under slicing-impact loading," *AIAA journal*, Vol. 52, No. 12, pp. 2701-2711.
- [20] Dias, J. A. C., Marqui, C. De and Erturk, A., 2015, "Three-degree-of freedom hybrid piezoelectric-inductive aeroelastic energy harvester exploiting a control surface" *AIAA journal*, Vol. 53, No. 2, pp. 394-404.
- [21] Scharpf, D. F. and Muleller, T. J., 1995, "An experimental investigation of the source of propeller noise due to the ingestion of turbulence at low speeds," *Experiments in Fluids*, Vol. 18, No., 4, pp 277-287.
- [22] Wojno, J. P., Muller, T. J. and Blake, W. K., 2002, "Rotor turbulence ingestion noise, part 1: experimental characterization of grid-generated turbulence," *AIAA journal*, Vol. 40, No. 1, pp. 16-25.
- [23] Wojno, J. P., Muller, T. J. and Blake, W. K., 2002, "Rotor turbulence ingestion noise, part 2: rotor acoustic response," *AIAA journal*, Vol. 40, No. 1, pp. 26-32.
- [24] Anderson, A. M., Catlett, M. R. and Stewart, D. O., 2015, "Modeling rotor unsteady forces and sound due to homogeneous turbulence ingestion," *AIAA journal*, Vol. 53, No. 1, pp. 81-92.
- [25] Atassi, M. H. and Atassi, O., 2004, "Nonreflecting boundary conditions for the time-dependent convective wave equation in a duct," *Journal of computational physics*, Vol. 197, Issue 2, pp. 737-758.
- [26] Attasi, H., Ali, A., Atassi, O. and Vinogradov, I., 2005, "Scattering of incident disturbance by an annular cascade in a swirling flow" *Journal of fluid mechanics*, vol. 499, pp. 111-138.
- [27] Atassi, O. and Ali, A., 2002, "Inflow/outflow condition for time-harmonic internal flows", *Journal of computational acoustic*, Vol. 10, pp.155-182
- [28] Vinogradov, I. And Zhou, Y., 2015, "Active control of rotor-stator interaction noise using stator-mounted actuators," *AIAA journal*, Vol. 53, No. 1, pp. 150-160.